JEM1068/ECE442 Laboratory Report

Lab Title/Number: Lab#5 Metal Deposition and Lift-Off

Group Number: 02

Instructor Name: Professor Wai Tung Ng, TNFC/ECE

Execution Date: October 20th, 2025

Report Submission Date: November 3rd, 2025

Submitted by: David Li, daviduoft.li@mail.utoronto.ca

Student Number: 1006940134

Contents

1. Executive Summary

This lab examines the microfabrication steps used to complete the process of fabricating the metal-oxide-semiconductor (MOS) capacitor on the highly doped silicon wafer. The capacitor dielectric is silicon dioxide. Subsequent to Labs #1 & #3, this lab's objective will focus on the deposition of the aluminum metal layer as a conductor plate and the formation of the final structure pattern from the "lift-off" process. Optical instrument is used to measure the layer thicknesses and electrical measurement is conducted for resistivity and thickness calculations. 25nm thick aluminum layer is deposited based on the sputter deposition recipe chosen.

2. Theoretical Background

2.1 Sputter Deposition

Metal is deposited onto the semiconductor surface by thermal, electron beam evaporation, or by sputter deposition, which is the method used in this lab. The material to be sputtered is called the target, in this case, aluminum. Sputtering is a process that use energetic particles such as Argon Ar^+ ions to bombard the target surface and as a result, particles sputtered out from the surface are deposited on to the substrate. This is a physical vapor deposition (PVD) technique. Sputter yield (S) represents the number of ejected target atoms for each incident ion, and relates to ion mass, ion energy, and other target properties. Fig 1 shows increase in sputter yield for larger ion energies.

	Argon					
	Yield at lowest ion energy					
Target	Y	E (ev)	100 (ev)	200 (ev)	300 (ev)	600 (ev)
Al	0.11	100	0.11	0.35	0.65	1.24

Fig 1. Sputtering Yield for Al under Argon ion bombardment [8]

The sputter removal rate (R_T) is based on the ion current and sputter yield.

$$R_T = \frac{I_p}{q} s \qquad (2.1.1)$$

The sputter deposition rate normal to the target surface will then be based on target to substrate distance D, and film growth rate can then be converted from this rate.

$$R(0) = \frac{R_T}{\pi D^2} \tag{2.1.2}$$

2.2 Lift-Off Patterning

The metal covers the entire surface of the wafer after the deposition process. The final metal pattern on the wafer is formed by lifting-off the metal that lies on top of the photoresist (PR). For positive PR, in this case S1818, commonly used stripper or remover is acetone. Since photoresist is removed in order to achieve metal lift-off, this process can be applied to any kind of metal. Regarding positive PR, modifications can be made for the cross-section of the PR after development to ensure PR stripper is in contact with the PR for remove, and detailed methods are outlined in [2].

2.3 Aluminum Thin Film Property

Aluminum is widely used metal for contacts, adhesion layers, and act as conductors in semiconductor processes. Thin film properties such as resistivity and phase are deeply connected with the deposition processes and recipes. In the deposition process in [9], there is a strong dependence of thin Al film (<50nm) resistivity on thickness as shown in Fig 2. Thin-film resistivity is usually much higher than bulk resistivity [1].

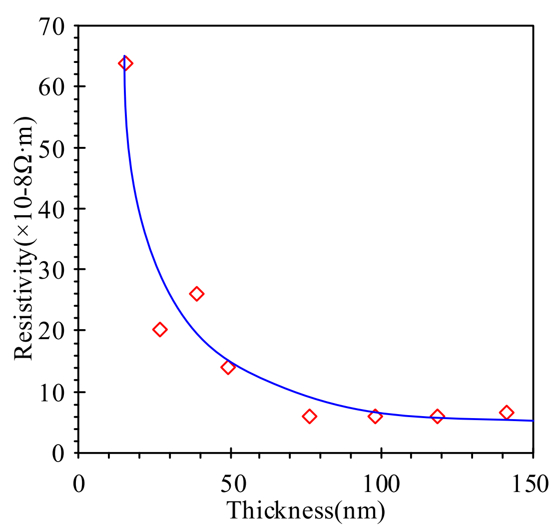

Fig 2. Electrical resistivity of sputter-deposited Al film [9]

2.4 Electrical Measurement

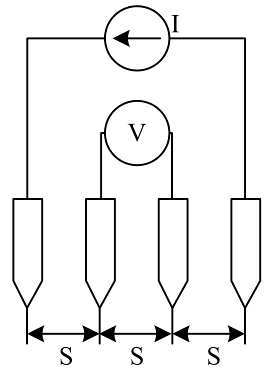

Fig 3. Four-Point Probe configuration [7]

The four-point probe (4PP) testing method is adopted as a metrology technique for sheet resistance for sputter-deposited metallic thin films. Physical contact is required from the tip of the probe to the measuring surface. The two outer probe needles are used to connect the current source and feed the current into the sample, and two inner probe needles are used to detect the voltage drop. Probe-tip spacings (s) of 0.5–2.0 mm is typical for semiconductor applications [7]. The resistance has the following formula and equals to the product of the sample resistivity and a geometrical factor. For resistivity ρ and thickness t, we have

$$R = \frac{V}{I} = \frac{\rho}{t} * g_4 \qquad (2.4.1)$$

$$g_4 = \frac{1}{\pi} \ln \frac{\sinh t/s}{\sinh t/2s} \qquad (2.4.2)$$

For thin layer, we have

$$\frac{t}{s} \ll 1 \quad g_4 \to \frac{\ln(2)}{\pi} \quad R = \frac{\ln(2)}{\pi} \frac{\rho}{t} \qquad (2.4.3)$$

The quantity of sheet resistance is a property of the particular layer (doping and thickness), and the units are given in ohms per square.

$$R_s = \frac{\rho}{t} \qquad (2.4.4)$$

3. Experimental Setup and Instruments

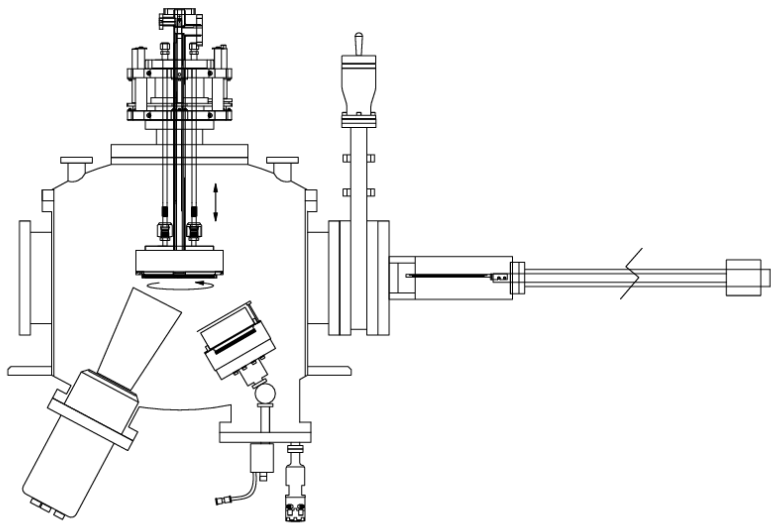

Fig 4. AJA ATC ORION Sputtering system [10]

AJA Sputter System is equipped with high vacuum magnetron sputtering sources and are powered by both RF generators and DC generators.

Fig 5. Four-Point Probe machine

Four Dimensions Four-Point Probe machine model 101C in Fig 5 is used in the lab to directly measure sheet resistance from the voltage and current values.

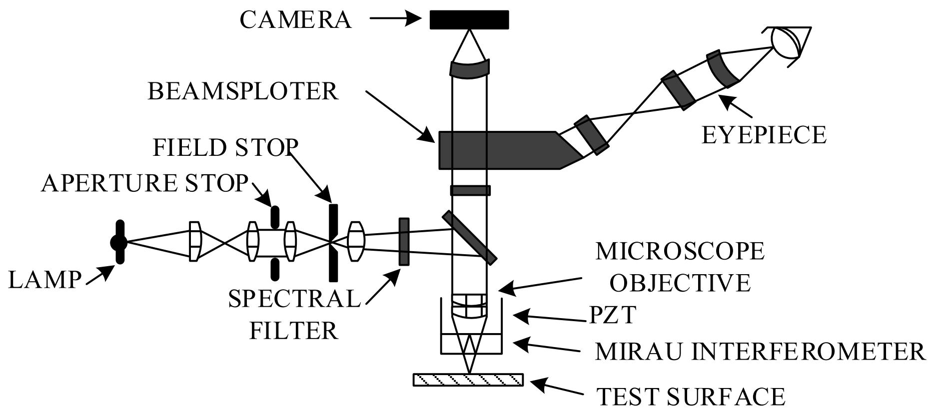

Fig 6. Schematic of interferometric optical profiler [6]

KLA Profile3D Optical Profilometer is a non-contact instrument that uses white light as the source for interference and incorporates both white light interferometry (WLI), and phase shifting interferometry (PSI) [5]. As shown in Fig 6. the light beam from the source reflects off of the wafer surface (rough) while another beam reflects off a reference surface in the Mirau interferometer. The interferogram produced due to different optical path length will result in the 3D surface topography map and 3D step heights (optical profilometry) can be measured. Based on the optical measurements, it can provide necessary information on wafer layer thicknesses (interferometry) due to sputter, deposition, or spin coating processes during manufacturing. Wide thickness range measurement from 50nm – 10mm is achieved with this profilometer [5].

Wetbench is used during cleaning and etch/lift-off processes. Isopropyl Alcohol (IPA) used as cleaning solvent. Acetone used to remove photoresist and Crystal bond

Optical Microscope is used to inspect the wafer after lift-off, and the metal contacts will be formed based on the openings in the mask pattern.

4. Experimental Procedure

Fabrication process steps are followed in the lab manual.

-Ensure Ar gas is turned on

-Roller set height to 20 and in Unlock position

-Record the pressure in the sputter chamber on the G937B Gauge Controller

-Load the sample and attach the sample to the holder using Kapton (polyimide) tape.

- Turn the load lock vacuum pump back on (power distribution module switch) to begin evacuating the load lock.

-Next is sample stage transfer, raise the substrate holder height to allow insertion of the transfer arm.

-Sputter Recipe is created in the AJA Phase II J computer control interface and selecting Gun3 RF200W.

-Once completed, wafer is used for probe testing for the thin film.

-Wafer is transferred to wetbench and placed in glass dish with acetone.

-wafer is dried in DI water and ready for pattern inspection.

5. Results

Result table is presented below.

Table 1. Data from lab, second set of data are from the other lab session.

	Sputtering Time	Goal Al Thickness	Sheet Resistance	Al Thickness using bulk Resistivity*	Al Thickness using thin-film Resistivity*	Al Thickness from Profiler
Our Session	360 s	25nm	4.23 ohm/sqr	6.26nm	23.64nm	140nm (optical)
Other Session	700 s	50nm	3.30 ohm/sqr	8.03nm	42.42nm	74.1-75.3nm (contact)

*noted the calculated values using equation 2.4.4 in the Appendix 1

Table 2. Sputter Deposition Recipe for both lab sessions

Target	Gun #	Pressure	Gas Flow	RF Power	Recipe deposition rate
Al	3	3 mTorr	30 AR	200 W	0.7 A/s

Fig 7. Starting wafer with 530nm LPCVD Oxide

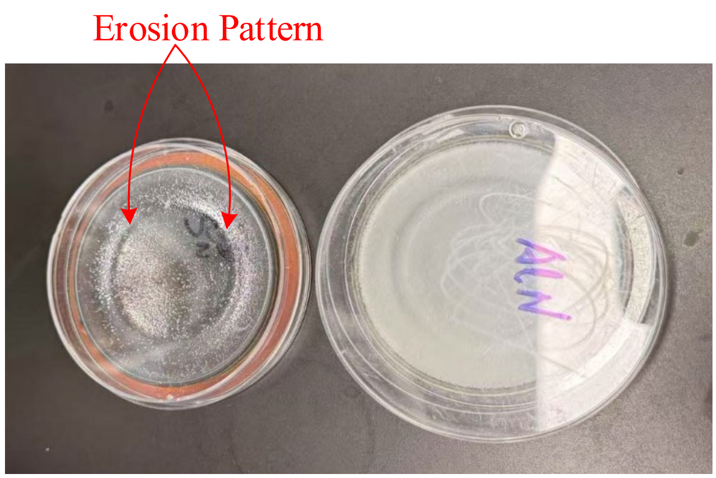

Fig 8. Used Aluminum magnetron target exhibiting erosion pattern

6. Discussion

As shown in Table 1, the aluminum thin film thickness calculated using aluminum bulk resistivity at room temperature gives the lowest thickness value compared to the target based on the recipe. This is due to the fact that thin-film properties such as resistivity, dielectric constant and other characteristics are thickness dependent. Although for aluminum, the thin-film resistivity is close to bulk value [1], it can be seen from [9] that for thin films less than 50nm, the resistivity is factor of two or higher. By selecting resistivity values based on [9]'s sputter deposition process of aluminum on silicon, thickness is calculated closer to the target value. However, it should be noted that different deposition system/machine results in different thin-film properties and that the underlying material (Si, SiO_2, etc.) also has an effect on film thickness [1].

Thickness should be measured independently, and sharp step was measured based on the optical profilometer. The height measurement was not accurate as mentioned in the announcement. Potential errors in PSI with white light could be camera nonlinearities, quantization or phase shifter errors, and vibration or air turbulence [11]. Reliability and repeatability results for thickness measurement comes from contact stylus profiler [3]. This measurement was not conducted during the lab session but was stated in the announcement for the other group section's data. The height of the liftoff aluminum is 74.1-75.3nm.

For aluminum target in magnetron plasma, with 200W power, the sputter yield at 10keV Ar^+ on aluminum is approximated to 3 atoms/ion in Fig 9 below. The sputter removal rate and subsequent aluminum film growth rate is calculated in Appendix 2, which results in 0.67 A/s, close to the recipe rate.

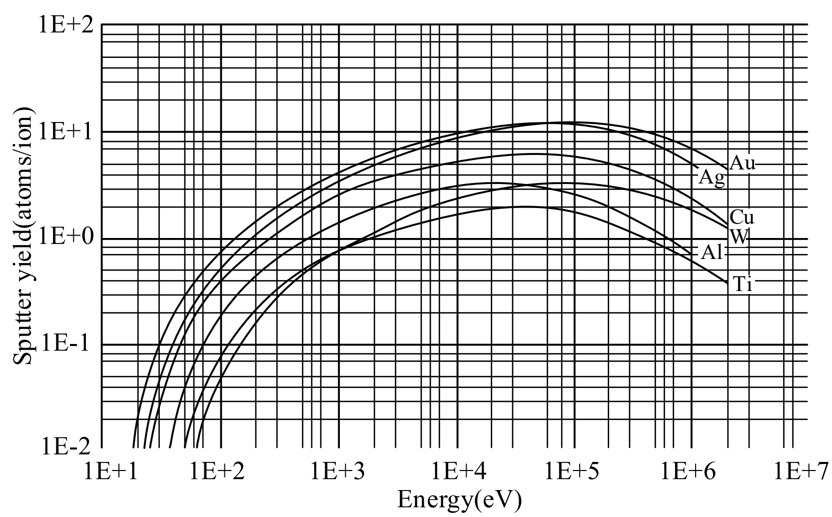

Fig 9. Calculated Ar^+ Sputter Yield curve for metals [3]

Due to the magnetron sputtering sources, the plasma density is greater at the place where the magnetic filed is parallel to the cathode plate. Higher sputter rate on the target is observed in Fig 8 as a ring-shaped erosion pattern. Magnetrons are able to sustain a plasma at pressures of 1-10mT, whereas conventional DC plasmas require much higher-pressure level above 100 mT.

7. Conclusions

Film growth technique and thin film properties have been studied in this lab. In particular, aluminum was deposited onto the wafer to form MOS capacitors. Measurements were performed for film thickness and device dimensions. Trade-offs between temperature, time, and deposition systems result in different thin-film properties. Metrology instruments should provide the most accurate data when interpreted correctly, especially when dealing with multilayer films. Future physical and chemical analysis can be performed to the sample using Scanning Transmission Electron Microscope under higher magnification to examine top view as well as cross-section for defects.

8. References

1. [1] S. Franssila, Introduction to microfabrication. Chichester, West Sussex, England: John Wiley & Sons, Inc., 2010, ch.5, pp.48-68.
2. [2] Y. Lian, Semiconductor microchips and fabrication: a practical guide to theory and manufacturing. Hoboken, New Jersey: John Wiley & Sons, Inc., 2023, ch.16, pp.225-244.
3. [3] A. Sarangan, Nanofabrication: Principles to Laboratory Practice. Boca Raton, Florida: CRC Press, 2019, ch.3, pp.53-98.
4. [4] TNFC_Lab #5 Metal Deposition and Lift-Off instruction manual, ECE442/JEM1068, 2025.
5. [5] Filmetrics® Profilm3D® Optical Profiler Specifications Sheet.
6. [6] James C. Wyant, Katherine Creath, Advances in interferometric optical profiling, International Journal of Machine Tools and Manufacture, Volume 32, Issues 1–2, 1992, Pages 5-10.
7. [7] A. Simon, Handbook of Thin Film Deposition, 3rd Edition. William Andrew Publishing, 2012, ch.4, pp.55-88
8. [8] N. Laegreid, G. K. Wehner, Sputtering Yields of Metals for Ar+ and Ne+ Ions with Energies from 50 to 600 ev. J. Appl. Phys., 32, 365, 1961.
9. [9] A. Karoui, Aluminum Ultra Thin Film Grown by Physical Vapor Deposition for Solar Cell Electric Nanocontacts, The Electrochemical Society, 2011.

10. [10] AJA International, INC. Product Brochure Welcome To AJA International, Inc!
11. [11] K. Creath, Error Sources in Phase-Measuring Interferometry, SPIE Vol. 1720, 1992, pp.428-435.

9. Appendices

Appendix 1

$$t = \frac{\rho_{al}}{R_{\text{sheet}}} = \frac{2.65\times10^{-8}\,\Omega\cdot m}{4.23\Omega / D} = 6.26nm$$

$$t = \frac{\rho_{Al}}{R_{\text{sheet}}} = \frac{2.65\times10^{-8}\,\Omega\cdot m}{8.3\Omega / D} = 8.03nm$$

Using $\rho_{al} = 10\times10^{-8}$ for thickness of 25nm

$$t = \frac{10\times10^{-8}}{4.23} = 23.64nm$$

For 50nm, $\rho_{al} = 14\times10^{-8}$

$$t = \frac{14\times10^{-8}}{3.3} = 42.42nm$$

Appendix 2

10 kev $\quad S = 3 \quad I = \frac{200}{1000} = 0.02 \quad q = 1.602\times10^{-19}$

$$R_T = \frac{I}{q}\cdot S$$

$$= 3.745\times10^{17}$$

$$R(0) = \frac{R_T}{\pi D^2} \qquad \text{D = 17cm}$$

$$= 4.09\times10^{14} \text{ atoms / cm}^2\text{ / s}$$

film growth rate

$$r = \frac{4.09\times10^{14}}{\frac{2.7}{26.9}\times6.12\times10^{23}} \qquad D = 17\text{cm}$$

$$= 6.77\times10^{-9}\,\text{cm/s}$$

$$= 0.67\dot{\text{A}}/\text{s}$$